Drosophila Hfp negatively regulates *dmyc* and *stg* to inhibit cell proliferation

Leonie M. Quinn[1], Ross A. Dickins[1], Michelle Coombe[1], Gary R. Hime[2], David D. L. Bowtell[1,*] and Helena Richardson[2,*]

[1]Trescowthick Research Laboratories, Peter MacCallum Cancer Centre, St Andrew's Place, East Melbourne, VIC 3002 Australia
[2]ARC Centre of Excellence in Biotechnology and Development, University of Melbourne
*Authors for correspondence (e-mail: david.bowtell@petermac.org and helena.richardson@petermac.org)

Accepted 27 November 2003

Development 131, 1411-1423
Published by The Company of Biologists 2004
doi:10.1242/dev.01019

Summary

Mammalian FIR has dual roles in pre-mRNA splicing and in negative transcriptional control of *Myc*. Here we show that Half pint (Hfp), the *Drosophila* orthologue of FIR, inhibits cell proliferation in *Drosophila*. We find that Hfp overexpression potently inhibits G1/S progression, while *hfp* mutants display ectopic cell cycles. Hfp negatively regulates *dmyc* expression and function, as reducing the dose of *hfp* increases levels of *dmyc* mRNA and rescues defective oogenesis in *dmyc* hypomorphic flies. The G2-delay in *dmyc*-overexpressing cells is suppressed by halving the dosage of *hfp*, indicating that Hfp is also rate-limiting for G2-M progression. Consistent with this, the cycle 14 G2-arrest of *stg* mutant embryos is rescued by the *hfp* mutant. Analysis of *hfp* mutant clones revealed elevated levels of Stg protein, but no change in the level of *stg* mRNA, suggesting that hfp negatively regulates Stg via a post-transcriptional mechanism. Finally, ectopic activation of the *wingless* pathway, which is known to negatively regulate *dmyc* expression in the wing, results in an accumulation of Hfp protein. Our findings indicate that Hfp provides a critical molecular link between the developmental patterning signals induced by the *wingless* pathway and dMyc-regulated cell growth and proliferation.

Key words: *Drosophila*, Hfp, Cell proliferation

Introduction

Regulation of cell proliferation is critical for the accurate propagation of genetic material, and development of tissues and organs in a multicellular animal. When these controls fail, excessive cell proliferation can lead to the formation of tumours and developmental abnormalities. Here we show that Half pint (Hfp; pUf68 – FlyBase), the *Drosophila* orthologue of mammalian FBP interacting repressor (FIR), is required to inhibit cell cycle progression during *Drosophila* development.

FIR and its *Drosophila* orthologue Hfp have an evolutionarily conserved function in pre-mRNA splicing. Mammalian FIR was originally isolated as poly(U) binding splicing factor (PUF60), and together with the splicing factors p54 and U2AF, promotes RNA splicing in vitro (Page-McCaw et al., 1999). Furthermore, FIR directly interacts with U2AF65, the large subunit of U2AF (Poleev et al., 2000). FIR and U2AF65 have similar domain structures, including the multiple RNA-recognition motif (RRM) domains. The *Drosophila* homologue of FIR has a conserved role in regulating pre-mRNA splicing and is known as Half pint (Hfp) (Van Buskirk and Schupbach, 2002), dPUF68 (Page-McCaw et al., 1999) or pUbsf (http://flybase.bio.indiana.edu/). Hfp controls RNA splicing of several *Drosophila* ovarian genes, including *ovarian tumor* (*otu*) (Van Buskirk and Schupbach, 2002) (reviewed by Rio, 2002). The *hfp* mutant ovary phenotype, which includes defective germline proliferation that results in reduced numbers of germline cells per egg chamber, is rescued by re-expressing an appropriately spliced *otu* isoform (Van Buskirk and Schupbach, 2002). Therefore *Drosophila* Hfp, like its mammalian counterpart FIR, has an important role in tissue-specific regulation of alternative splicing.

In addition to regulating splicing of pre-mRNA, mammalian FIR is also an important regulator of *Myc* gene activity (Eisenman, 2001; Liu et al., 2000). Expression of *Myc* is tightly regulated, at the level of transcription, translation and protein stability (Eisenman, 2001). One mechanism for control of *Myc* transcriptional initiation and elongation is mediated by the far upstream element (FUSE), a DNA sequence located 1500 bp upstream of the *Myc* promoter. The FUSE binding protein (FBP), a KH domain transcriptional activator, binds the FUSE and is absolutely required for *Myc* expression and cell growth in mammalian cells (Duncan et al., 1994; He et al., 2000). The FBP interacting repressor (FIR) counteracts FBP function by forming a ternary complex with FBP and the FUSE to repress *Myc* transcription (Liu et al., 2000). The N-terminal repression domain of FIR interacts with the basal transcription component TFIIH and interferes with promoter clearance. The in vivo importance of this mechanism is not clear; however, mutations in *ERCC2* or *ERCC3* (which encode TFIIH subunits corresponding to the *xeroderma pigmentosum* (*XP*) complementation groups *XPD* and *XPB*, respectively) impair regulation of *Myc* expression by FBP and FIR. This may contribute to cancer risk in individuals with XP mutations (Liu et al., 2001).

The proteins encoded by the *myc* family of proto-oncogenes

are important regulators of cell growth (size and mass increase), proliferation, differentiation and apoptosis (Eisenman, 2001). In response to mitogenic signalling, Myc can inhibit differentiation and either promotes cell growth and proliferation or apoptosis, depending on the context. Myc proteins form stable heterodimers with Max proteins to modulate expression of target genes by binding E box DNA sequences. Although primarily a transcriptional activator, Myc can also inhibit the expression of certain target genes. Deregulated Myc expression is potently oncogenic and is one of the most frequently observed molecular abnormalities in human cancers. Despite this, regulation of Myc expression and its role in tumourigenesis has not been clearly defined.

The *Drosophila dmyc* (*dm* – FlyBase) and *dmax* (*Max* – FlyBase) gene products also form heterodimers, bind E-box DNA sequences and activate transcription (Eisenman, 2001; Gallant et al., 1996). Gain and loss of function studies in *Drosophila* have revealed that the primary in vivo function of dMyc is to stimulate cell growth. *dmyc* mutations cause cellular growth retardation; resulting in small flies with small cells (Gallant et al., 1996; Johnston and Edgar, 1998; Johnston et al., 1999; Schreiber-Agus et al., 1997). Conversely, overexpression of *dmyc* in the wing imaginal disc promotes cell growth, leading to increased cell size (Johnston et al., 1999). Although dMyc-induced cell growth is accompanied by faster G1/S phase progression, the overall cell division rate of *dmyc* overexpressing cells remains normal due to an extended G2 phase (Johnston et al., 1999), which arises because the *Drosophila* homologue of Cdc25 phosphatase, String (Stg), is rate limiting for G2-M cell cycle progression (Edgar and O'Farrell, 1989; Edgar and O'Farrell, 1990). Stg triggers mitotic entry by dephosphorylating, and thereby activating the Cdk1/Cyclin B kinase (Edgar et al., 1994).

The Wingless-signalling pathway regulates both *dmyc* and *stg* expression during *Drosophila* wing development. During third instar larval development, the dorsoventral compartment boundary of the wing imaginal disc forms a zone of cells arrested in G1 or G2, termed the ZNC. A band of Wingless (Wg) expression controls cell cycle arrest within the ZNC (Johnston and Edgar, 1998). While *dmyc* is expressed in proliferating zones within the wing, expression is normally low in the ZNC, and ectopic expression of *dmyc* in the ZNC prevents cell cycle exit (Johnston et al., 1999). Furthermore, inhibition of Wg signalling in the ZNC, via expression of dominant negative TCF, results in ectopic *dmyc* expression in the ZNC (Johnston et al., 1999). These studies show that Wg signalling represses *dmyc* expression within the ZNC; however, whether the repression of *dmyc* transcription by TCF is direct or indirect is unknown. While the posterior region of the ZNC is comprised solely of G1-arrested cells, the anterior compartment of the ZNC contains a band of G1-arrested cells at the dorsoventral boundary that is sandwiched between anterior–dorsal and anterior–ventral G2-arrested domains. Wg signalling is required for the downregulation of *stg* and associated G2-arrest in the anterior of the ZNC. This occurs indirectly, via Wg upregulating *achaete* and *scute*, which in turn downregulate *stg*, resulting in the G2-arrested cells in the ZNC (Johnston and Edgar, 1998). Whether Achaete and Scute act directly on the *stg* promoter is unknown.

Here we describe an alternative role for Hfp, as a negative regulator of cell cycle progression in *Drosophila* imaginal tissues. We show that within the ZNC of hypomorphic *hfp* mutant wing discs, cells undergo ectopic S phases, suggesting that, like FIR, Hfp might control cell proliferation by regulating *dmyc* expression. Indeed, elevated *dmyc* expression was detected in *hfp* mutant clones, and reducing the dosage of *hfp* rescued the *dmyc* mutant ovary phenotype. Unlike *dmyc* overexpression, *hfp* mutants did not affect cell growth, although cell proliferation was increased. This can be explained via an affect of Hfp on the G2-M phase transition, since *hfp* mutants can rescue the cycle 14 G2-arrest phenotype of an *stg* mutant. Furthermore, Hfp protein was elevated in response to Wg pathway signalling. Taken together, these results are consistent with Hfp playing an important role in cell cycle arrest downstream of Wg signalling. These findings suggest that Hfp links patterning signals to cell growth and proliferation in the *Drosophila* wing.

Materials and methods

Fly strains and generation of transgenic flies

Since the *hfp* mutant strain *EP3058* contained additional lethal mutations (Van Buskirk and Schupbach, 2002), recombination was used to isolate the hfp^{EP} allele. The purified hfp^{EP} failed to complement deficiency *Df(3L)Ar14-8*, which has breakpoints 61C4-62A8 covering *hfp* (Van Buskirk and Schupbach, 2002). To generate the *UAS-hfp* construct, full-length *hfp* cDNA was subcloned into *pUAST* and transgenic flies were generated as previously described (Richardson et al., 1995). *UAS-hfp* transgenes on the second and third chromosomes were used for all experiments. Recombinants of *GMR-GAL4* and *UAS-hfp* on the second chromosome were used to test for genetic interactions at 25°C. Recombinants of hfp^{EP} and stg^{AR2} were generated and balanced over *TM6B, abdA-lacZ*, and double-mutant embryos were selected based on the absence of AbdA-LacZ staining. All general fly stocks were obtained from the Bloomington Stock Centre, except the $UAS\text{-}TCF^{DN}$ and *en-GAL4,UAS-GFP* (from Laura Johnston), *axin*, *FRT82B* (from Jessica Treisman), *C96-GAL4* (from Bruce Edgar) and *GMR-p21* (from Iswar Hariharan). For analysis of clones *hs-FLP*; *FRT80B, Tb-GFP* females were crossed to *FRT80B*, hfp^{EP}/*TM6B* males, clones were generated by heat shocking (at 37°C for 1 hour) second instar larvae and wandering third instar larvae were dissected and analysed. Similarly, *axin* clones were generated by crossing *hs-FLP*; *FRT82B, Ub-GFP* females to *FRT82B, axin*/*TM6B* males.

In-situ hybridization, antibody staining, BrdU and TUNEL labelling and microscopy

mRNA in-situ hybridization was carried out as described in previous methods (Dorstyn et al., 1999) except the signal was detected using fast-red substrate (Roche). Following in-situ hybridization, clones were distinguished using a rabbit anti-GFP polyclonal antibody (Molecular Probes), detected using an anti-rabbit-biotin conjugated secondary antibody, followed by streptavidin-Alexa488 (Molecular Probes). After in-situ hybridization of ovaries, DNA staining was carried out with Oligreen (Molecular Probes) to assist with staging.

Immunohistochemistry, including TUNEL and BrdU labelling of *Drosophila* larval tissues and embryos, was carried out as previously described unless otherwise indicated (Quinn et al., 2000; Quinn et al., 2001). The monoclonal Hfp antibody (Trudi Schupbach) was detected using an anti-mouse-biotin conjugated secondary antibody followed by streptavidin-lissamine rhodamine (Jackson). TUNEL staining was carried out using the in-situ cell death detection kit TRred (Roche). Other antibodies used were anti-BrdU monoclonal antibody (Becton Dickinson) and rabbit anti-phosphohistone H3 (Santa Cruz), rabbit anti-GFP (Molecular Probes), rabbit anti-Cyclin B (David Glover), rat anti-Geminin (Quinn et al., 2001), rabbit anti-βgal (Rockland) and

rabbit anti-Stg (Bruce Edgar). Ovaries were stained with phalloidin-rhodamine, 0.1% in PBT for 1 hour (Sigma), prior to staining with Oligreen (Molecular Probes). All fluorescently labelled samples were analysed by confocal microscopy (Biorad MRC1000). Scanning electron micrographs of adult eyes were generated as previously described using a Field Emission Scanning Electron Microscope (Secombe et al., 1998).

Results

Mutation of *hfp* affects cell proliferation and larval growth

The *Drosophila* stock *EP(3)3058* (hfp^{EP}) harbours a recessive lethal *P* element insertion in the 5′ UTR of *hfp*, 94 bp upstream of the initiating methionine codon (Van Buskirk and Schupbach, 2002). Homozygous hfp^{EP} larvae were of similar size to age-matched wild type third instar larvae. However, the pupariation of hfp^{EP} larvae was consistently delayed by approximately 2 days, and continued growth during this period resulted in wandering larvae and pupae ~20% larger than wild-type third instar larvae (Fig. 1A,C). The duration of the pupal stage was normal for hfp^{EP} mutant animals; however, they failed to eclose and died as pharate adults that were larger than wild type (Fig. 1B). The hfp^{EP}/hfp^{EP} terminal phenotype included duplication of superior scutellar macrochaete, and malformation of legs, wings and sex combs (data not shown).

The pleiotropic phenotype of *hfp* mutant animals indicated that Hfp might be involved in several stages of development. In *Drosophila*, maternal transcripts are transferred during oogenesis and serve to sustain early embryonic development until stage 5, after which zygotic transcription commences. Northern analysis revealed that *hfp* mRNA was maternally deposited in the early embryo; however, zygotic *hfp* expression was low during late embryonic and early larval stages (Fig. 1D). *hfp* transcripts were also detected in third instar larvae, pupae and adults. We observed a marked decrease in *hfp* mRNA in hfp^{EP}/hfp^{EP} and hfp^{EP}/*Df(3L)Ar14-8* larvae compared with age-matched wild-type third instar larvae (Fig. 1E). However, *hfp* transcript was still detectable, consistent with the notion that hfp^{EP} is not a null allele (Van Buskirk and Schupbach, 2002). In wild-type animals, expression of *hfp* during third instar (Fig. 1D) coincides with the onset of differentiation in imaginal discs. We examined Hfp protein expression in wing discs using an antibody recognizing Hfp (Van Buskirk and Schupbach, 2002) and used an antibody to Geminin, which is abundant in late S phase and G2 but absent in G1 cells (Quinn et al., 2001), to visualize the ZNC (Fig. 1F; see Introduction). Hfp protein was detected in the nucleus of most wing disc cells, with higher staining in cells in the ZNC (Fig. 1G). Consistent with northern analysis, Hfp protein level was significantly reduced in wing discs from hfp^{EP}/hfp^{EP} larvae (Fig. 1H).

In order to investigate whether Hfp regulates cell proliferation during *Drosophila* development, we measured BrdU incorporation in wing discs from wandering hfp^{EP}/hfp^{EP} larvae. In wild-type wing discs the ZNC is clearly marked by the absence of BrdU labelling (Fig. 1I). The number of S-phase cells was markedly increased in hfp^{EP} mutant wing discs, BrdU incorporation was uniform across the disc and cell cycle arrest was not evident in the ZNC region (Fig. 1L). Strikingly, anti-phosphohistone H3 antibody staining of mitotic cells (Hans and Dimitrov, 2001), was also elevated, indicating an overall increase in cell proliferation in *hfp* wing discs (Fig. 1M; 127±7 mitotic cells per disc) compared with wild type (Fig. 1J; 75±8 mitotic cells; n=5 discs, P<0.01).

The developing eye is a sensitive system for analysis of cell proliferation. During wild-type eye development, a wave of differentiation moves from posterior to anterior across the third instar eye imaginal disc. Within the morphogenetic furrow (MF) cells are arrested in G1 and posterior to the MF a subset of cells enter a synchronous S phase (Fig. 1O) while other cells begin differentiation to form ommatidial pre-clusters, followed by a band of mitotic cells known as the second mitotic wave (Fig. 1P). Analysis of the band of S phases posterior of the MF (Fig. 1R) and the second mitotic wave (Fig. 1S) in *hfp* mutant eye discs revealed that the S-phase band is generally broader than for wild type, but the second mitotic wave does not occur prematurely, suggesting that Hfp might normally be required for the pre-cluster cells to cease division.

Despite increased proliferation in hfp^{EP} mutant discs, they were not overgrown compared with wild type (data not shown). We did not observe an obvious difference in cell size between hfp^{EP} mutant wing disc cells by either cross section (Fig. 1V compared with wild type, Fig. 1U) or by transverse section (data not shown), suggesting that increased cell death may accompany increased proliferation in this tissue to account for the fact that the discs are similar in size to wild type. Indeed, TUNEL staining revealed an increase in the number of apoptotic cells in the wing imaginal discs of *hfp* mutants (Fig. 1X; 143±17 apoptotic cells per disc) compared with wild-type larvae (Fig. 1W; 26±9 apoptotic cells, n=5 discs, P<0.005).

Therefore, although increased cell cycles were observed in *hfp* mutant wing discs, the overall disc size was similar to wild type, as ectopic proliferation was apparently balanced by increased apoptosis. The elevated cell death observed in *hfp* mutant wing discs is likely to be a secondary consequence of deregulated cell proliferation. In *Drosophila*, compensatory cell death in the face of hyperproliferation appears to be a general mechanism for maintaining normal compartment size and is also observed in imaginal discs upon ectopic expression of *dmyc* (Johnston et al., 1999), the cell cycle transcription factor E2F (Asano et al., 1996) or both the G1-S phase regulator Cyclin E and the G2-M phase regulator Cdc25/Stg (Neufeld et al., 1998).

Hfp overexpression inhibits cell cycle entry

The observation that loss of Hfp promotes cell cycle entry prompted us to examine whether overexpression of Hfp could block cell proliferation. We generated transgenic flies containing a *UAS-hfp* transgene in order to ectopically express Hfp using various *GAL4* drivers (Brand and Perrimon, 1993). Ubiquitous expression of Hfp using *armadillo-GAL4* (*arm-GAL4*) partially rescued the pupal lethality of hfp^{EP}/hfp^{EP} animals, verifying transgene function (data not shown). We specifically overexpressed *hfp* in cells posterior to the MF in the eye disc using the *GMR-GAL4* driver. Expression of two copies of *UAS-hfp* under control of *GMR-GAL4* (*GMR-GAL4,UAS-hfp*/+; *UAS-hfp*/+) resulted in flies with disorganized adult eyes that were slightly smaller than wild type (Fig. 2B). Third instar eye discs from *GMR-GAL4,UAS-hfp*/+; *UAS-hfp*/+ larvae showed reduced BrdU incorporation in the S-phase band posterior to the MF (Fig. 2D) compared with wild type (Fig. 2C). In addition, reduced numbers of cells

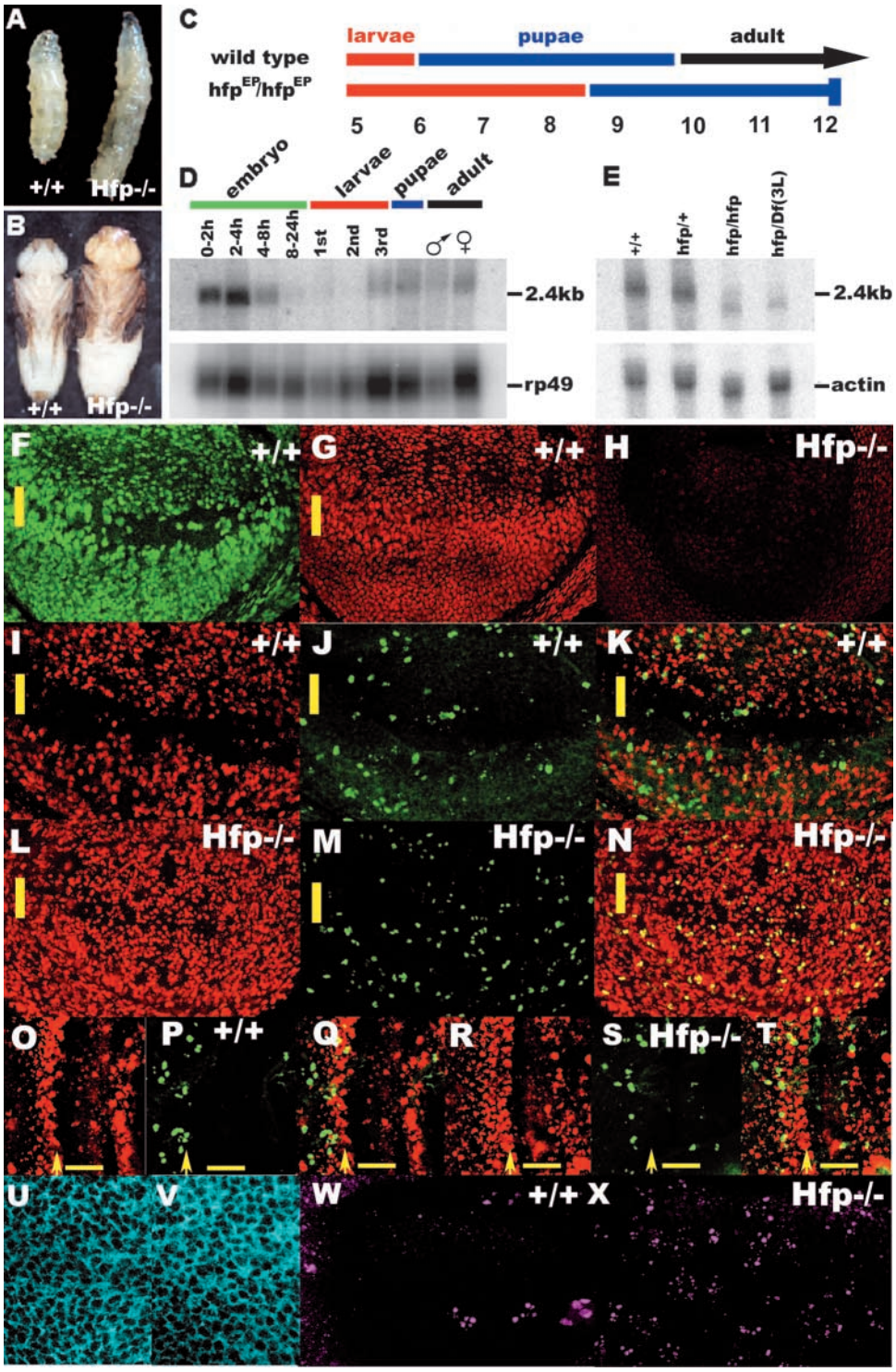

Fig. 1. Hfp negatively regulates cell cycle progression. (A) A wild-type third instar larva (left) alongside an hfp^{EP}/hfp^{EP} late third instar larva (right). (B) A wild-type pharate adult (left) alongside a hfp^{EP}/hfp^{EP} pharate adult (terminal phenotype; right). (C) Time line of the developmental delay observed in hfp^{EP}/hfp^{EP} animals compared with wild type. The vertical bar indicates the stage at which *hfp* mutants arrest in development and die. (D) Northern blot of poly(A)+ RNA isolated from the developmental stages shown, and probed with the *hfp* cDNA, then stripped and re-probed with the ribosomal protein *rp49* cDNA as a loading control. (E) Northern blot of poly(A)+ RNA isolated from wild-type and *hfp* mutant larvae, probed with the *hfp* cDNA and *Actin5c* cDNA as a loading control. (F-N) Wing imaginal discs from wandering third instar larvae. Posterior is to the right, and the left margin of the ZNC is marked with a yellow bar. Discs shown are representative samples of at least 30 discs examined for each condition. (F,G) Wild type disc co-stained with anti-Geminin antibody (F) and anti-Hfp antibody (G). Geminin is present in late S-phase and G2 cells, but absent from G1-arrested cells (Quinn et al., 2001). (H) Anti-Hfp antibody staining of a hfp^{EP}/hfp^{EP} larval wing disc. (I-N) Wing discs from wild type (I-K) and hfp^{EP}/hfp^{EP} (L-N) larvae co-labelled with BrdU (I,L), anti-phosphohistone H3 antibody (PH3) (J,M) or merged (K,N). (O-T) Third instar eye imaginal discs from wild-type (O-Q) and hfp^{EP}/hfp^{EP} (R-T) larvae co-labelled with BrdU (O,R), PH3 (P,S) or merged (Q,T). The morphogenetic furrow (MF) is indicated by a yellow bar and arrows indicate the normal position of the S-phase band posterior to the MF. (U,V) Cell size visualized by spectrin staining of wild type (U) and hfp^{EP}/hfp^{EP} (V) wing discs. (W,X) TUNEL staining of wild-type (W) and hfp^{EP}/hfp^{EP} (X) wing discs, revealing elevated apoptosis in *hfp* mutant tissue.

staining with anti-phosphohistone H3 were observed posterior to the S-phase band of *GMR-GAL4,UAS-hfp*/+; *UAS-hfp*/+ eye discs (Fig. 2F) compared with wild type (Fig. 2E). Thus overexpression of *hfp* can inhibit S phase entry and mitoses posterior to the MF, consistent with a role for Hfp in negatively regulating cell cycle progression.

We then examined the effect of overexpressing *hfp* in the wing disc by using *engrailed-GAL4* (*en-GAL4*), which drives transgene expression in the posterior compartment of the wing disc (Kornberg et al., 1985). Defects were observed in the posterior wing compartment in *en-GAL4; UAS-hfp/+* adults. The phenotype varied in severity from slight wing vein abnormalities and decreased wing size (Fig. 2H and 2I) to disrupted, small and blistered wings (Fig. 2J). To analyse wing discs, the posterior compartment of third instar larval wing discs was marked by co-expression of a *UAS-GFP* transgene with the *en-GAL4* driver. The posterior wing compartment overexpressing *hfp* was small compared with the wild type

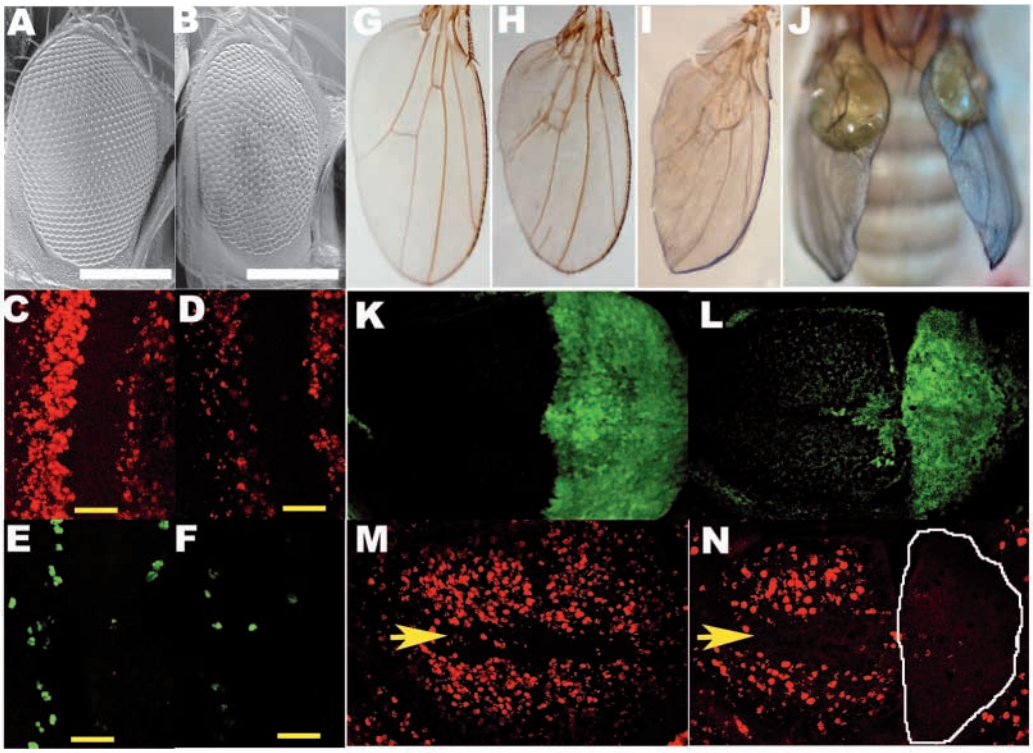

Fig. 2. Overexpression of *hfp* inhibits cell cycle entry in the developing eye and wing. (A,B) Scanning electron micrographs of adult eyes of wild type (A) and *GMR-GAL4, UAS-hfp/+; UAS-hfp/+* (B). Scale bar equals 200 μm. (C-F) Eye imaginal discs from wild type (C,E) and *GMR-GAL4,UAS-hfp/+; UAS-hfp/+* (D,F) third instar larvae, co-labelled with BrdU (C,D) and anti-phosphohistone H3 antibody (E,F). Posterior is to the left. Yellow bars indicate the MF. (G-J) Adult wings mounted in Canada balsam (G-I) or fresh (J) from *en-GAL4,UAS-GFP* (G) and *en-GAL4,UAS-GFP/+,UAS-hfp/+* (H-J) flies. (K-N) Third instar wing discs from *en-GAL4,UAS-GFP* (K,M) and *en-GAL4,UAS-GFP/+,UAS-hfp/+* (L,N) flies, co-labelled using GFP antibody staining to mark the posterior region of the wing disc (K,L) and BrdU (M,N). The ZNC is marked with an arrow, and in (N) the GFP-positive region is outlined in white.

posterior wing compartment (compare GFP in Fig. 2L with wild type in Fig. 2K). As the phenotype resulting from overexpression of the *hfp* transgene with the *en-GAL4* driver was slightly variable, presumably as a consequence of subtle variations in the level of transgene expression, we evaluated the reduction in compartment size by comparing the area of the posterior compartment of *en-GAL4,UAS-GFP/+; UAS-hfp/+* wing discs with the same from control *en-GAL4,UAS-GFP*. As the area corresponding to the posterior compartment of the wing is marked by GFP in each case, we used this to determine that Hfp overexpressing tissue was reduced by 31.7% (mean of the average number of pixels=66,931±19247; n=5) compared with the control (mean of the average number of pixels=96,616±7566; n=5). The region surrounding the ZNC of the wing disc is normally highly proliferative (Fig. 2M); however, overexpression of Hfp in the posterior compartment of the wing resulted in fewer BrdU-labelling cells (Fig. 2N). Thus overexpression of *hfp* in either eye or wing imaginal discs results in cell cycle inhibition and is associated with reduced overall size of these tissues. Taken together with the loss-of-function studies (above) these findings suggest that Hfp normally functions to inhibit cell cycle progression.

Loss of *hfp* suppresses the cell cycle inhibitory affects of p21/Dacapo

Overexpression of human p21 (an inhibitor of G1-S cyclin-dependent kinases) posterior to the MF, under the control of the *GMR* promoter, inhibits S-phase entry posterior to the MF and results in a rough eye phenotype in adults (de Nooij and Hariharan, 1995). The *GMR-p21* rough eye phenotype can be modified by reducing the dose of cell cycle regulators (Secombe et al., 1998), providing a sensitive system to investigate the role of putative cell cycle regulators. When the dosage of *hfp* was reduced in a *GMR-p21* background, the rough adult eye phenotype was dominantly suppressed; *GMR-p21*/+, hfp^{EP}/+ eyes were larger and contained fewer fused ommatidia (Fig. 3C) than *GMR-p21*/+, +/+ eyes (Fig. 3B). Similarly, we found that the mild rough eye phenotype caused by overexpression of the *Drosophila* p21/p27 homologue *dacapo (dap)* was dominantly suppressed by mutation in *hfp* (data not shown).

In third instar larval eye discs, *GMR-p21* abolishes the band of S phases posterior to the MF and the second mitotic wave (Fig. 3E,H,K). Compared with *GMR-p21*/+, eye discs from *GMR-p21*/+, hfp^{EP}/+ contained more S-phase cells posterior to the MF (Fig. 3F compared with 3E), and an accompanying increase in mitotic cells (Fig. 3I compared with 3H). Thus, the dominant suppression of the *GMR-p21* rough eye phenotype by hfp^{EP} can be explained by this partial rescue of cell proliferation in the eye imaginal disc. These results, together with the analysis of hfp^{EP}/hfp^{EP} wing discs, suggest that Hfp inhibits cell cycle entry in larval imaginal discs.

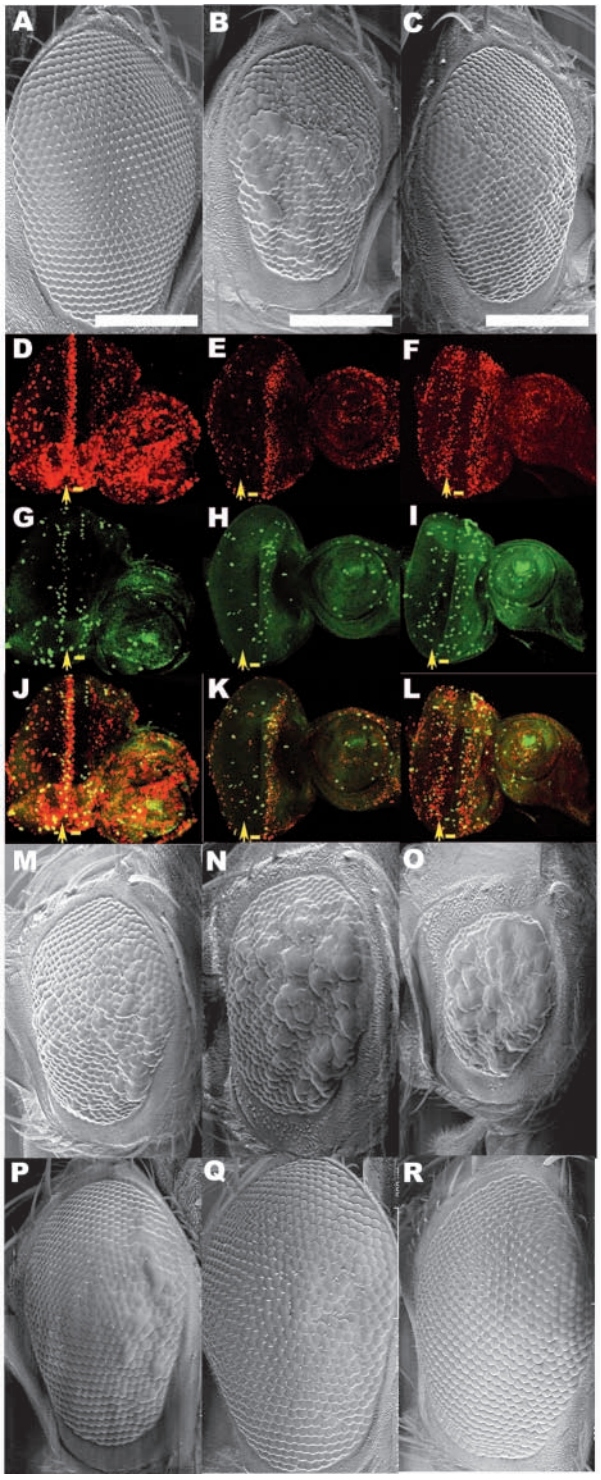

Fig. 3. *hfp* mutation suppresses the *GMR-p21* eye phenotype by promoting cell cycle entry. (A-C) Scanning electron micrographs of adult eyes from wild-type (A), *GMR-p21/+* (B) and *GMR-p21/+*; hfp^{EP}/+ (C) flies. Scale bar equals 200 μm. (D-L) Eye imaginal discs from wild-type (D,G,J), *GMR-p21/+* (E,H,K) and *GMR-p21/+*; hfp^{EP}/+ (F,I,L) larvae, co-labelled with BrdU (D-F) and PH3 antibody (G-I). Merged images are shown (J-L). Posterior is to the left. The MF is indicated by a yellow bar and arrows indicate the normal position of the S-phase band posterior to the MF. (M-R) Scanning electron micrographs of adult eyes, to show genetic interactions between p21/Dacapo and dMyc; (M) *GMR-p21/+* males, (N) *dmycP0/+*;*GMR-p21/+* females, (O) *dmycP0/y*; *GMR-p21/+* males, (P) *GMR-GAL4/+*, *UAS-dacapo/+*, (Q) *GMR-GAL4/+*; *UAS-dmyc/+*, (R) *GMR-GAL4/+*, *UAS-dacapo/+*; *UAS-dmyc/+*.

Given that mammalian FIR protein negatively regulates the cell cycle via *Myc*, and the above data showing that Hfp might normally inhibit cell cycle progression through p21/Dacapo, we tested *Drosophila* Myc (dMyc) for genetic interactions with p21/Dacapo. The dMyc mutant enhances the *GMR-p21* phenotype (Fig. 3N females of genotype $dmyc^{P0}$/+;*GMR-p21/+* and Fig. 3O males $dmyc^{P0}$/*Y*; *GMR-p21/+* compared with the control female *GMR-p21/+*, in Fig. 3M). Conversely, the *GMR-GAL4, UAS-dacapo* reduced/rough eye phenotype is suppressed by co-expression of a *UAS-dmyc* transgene (Fig. 3R compared with Fig. 3P). The finding that the inhibitory affect of p21/Dacapo on the G1 to S transition can be suppressed by either reducing the dose of *hfp* or by overexpressing *dmyc*, suggests that Hfp and dMyc may have antagonistic effects on the G1 to S transition in the eye imaginal disc.

Mutation of *hfp* rescues the ovary phenotype and sterility of *dmyc* mutant females

Given that mammalian FIR protein is a negative regulator of *Myc*, and the above data showing that Hfp inhibits cell cycle progression, we investigated the possibility that Hfp regulates *dmyc* in *Drosophila*. If the role of Hfp as a negative regulator of *dmyc* has been conserved, we hypothesized that reducing the dose of *hfp* might suppress the *dmyc* mutant phenotype. The three characterized hypomorphic *dmyc* alleles, *diminutive*[1] ($dmyc^{dm1}$) (Gallant et al., 1996), $dmyc^{P0}$, and $dmyc^{P1}$, are all recessive female sterile (unpublished data). Analysis of ovaries from $dmyc^{P0}$ and $dmyc^{P1}$ females revealed that early stage (stage 2-9) egg chambers were of normal appearance but then arrested between stages 10-11 of oogenesis with smaller ovarioles (Fig. 4B,D).

Progression beyond stage 10 of oogenesis requires dumping of the nurse cell cytoplasm into the oocyte, which is followed by nurse cell apoptosis (Buszczak and Cooley, 2000). An initial step of dumping is formation of dense bundles of actin filaments in the nurse cell cytoplasm, essential for structural support of nurse cell nuclei (Gutzeit, 1986). Although actin filaments were present in stage 10 $dmyc^{P0}$/$dmyc^{P0}$ egg chambers (Fig. 4B compared with Fig. 4A), cytoplasmic actin bundles failed to develop around stage 11 nurse cell nuclei (Fig. 4D compared with Fig. 4C). Thus $dmyc^{P0}$/$dmyc^{P0}$ ovaries fail to undergo nurse cell death, which is required for progression to stage 12 of oogenesis (Fig. 4G compared with Fig. 4F, and measured by TUNEL, data not shown). Strikingly, the hfp^{EP} mutation dominantly suppressed these defects in $dmyc^{P0}$/$dmyc^{P0}$ ovaries (Fig. 4E,H). The actin network appeared normal in nurse cells from stage 10 $dmyc^{P0}$/$dmyc^{P0}$; hfp^{EP}/+ ovaries (Fig. 4E), and TUNEL positive nuclei were obvious at stage 12 (data not shown). Indeed $dmyc^{P0}$/$dmyc^{P0}$; hfp^{EP}/+ and $dmyc^{P1}$/$dmyc^{P1}$; hfp^{EP}/+ females yielded mature oocytes (Fig. 4H) that gave rise to viable embryos (data not shown).

DNA endoreplication in nurse cells and follicle cells also occurs during stage 10 of oogenesis. Follicle cells undergo

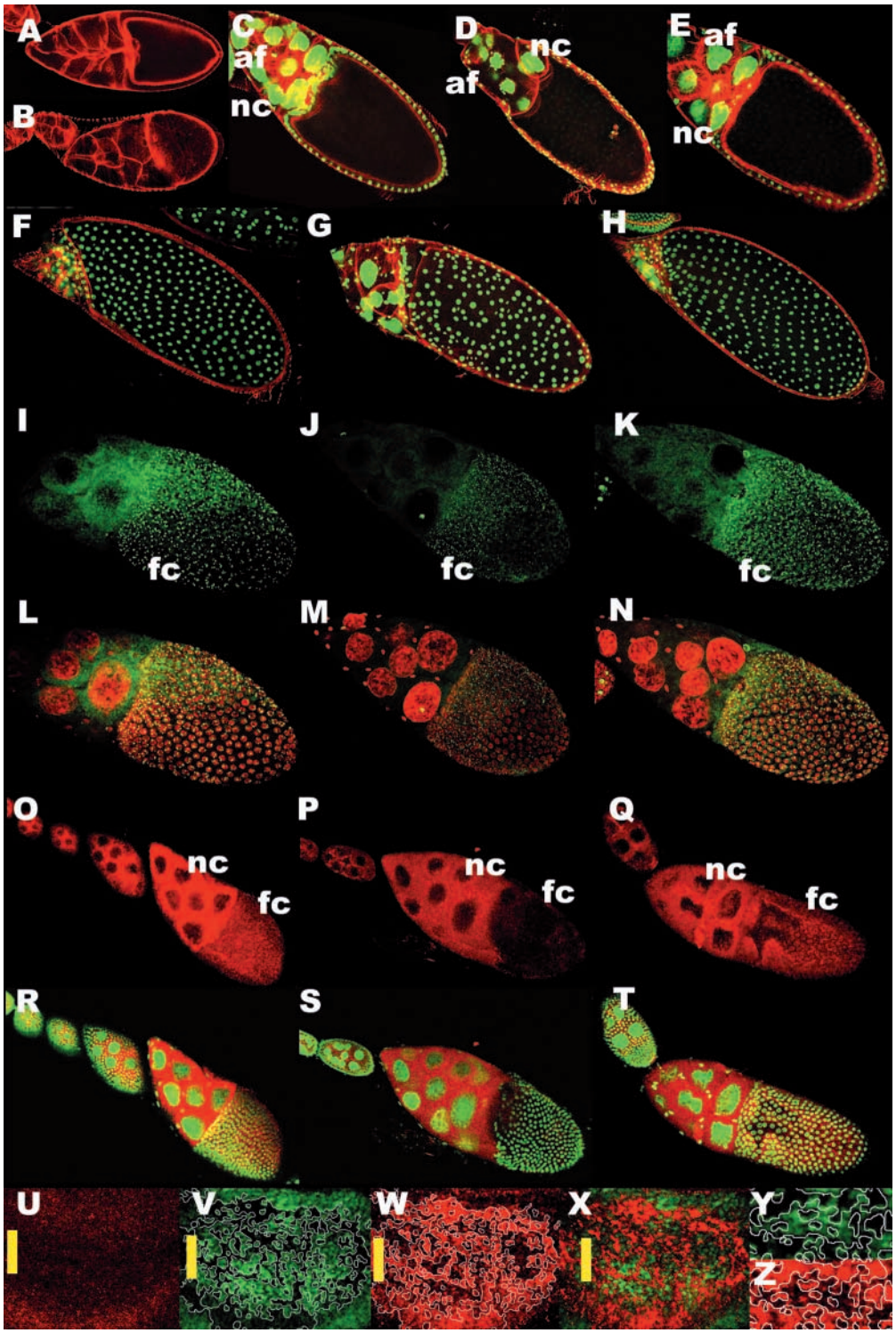

Fig. 4. *hfp*^{EP} dominantly suppresses the *dmyc* mutant ovary phenotype and *dmyc* expression is increased in *hfp* mutant clones. (A-T) All ovarioles are oriented with the most mature/posterior egg chamber to the right. nc=nurse cells, af=actin filament bundles, fc=follicle cells. (A-B) Ovaries stained with phalloidin (red) to show filamentous actin and (C-H) with phalloidin and the DNA stain Oligreen. Egg chamber genotypes and stages: wild-type stage 10 (A), *dmyc*^{P0}/*dmyc*^{P0} stage 10 (B), wild-type stage 11 (C), *dmyc*^{P0}/*dmyc*^{P0} stage 11 (D), *dmyc*^{P0}/*dmyc*^{P0}; *hfp*^{EP}/+ stage 11 (E), wild-type stage 14 (F), *dmyc*^{P0}/*dmyc*^{P0} arrested at stage 11 (G), *dmyc*^{P0}/*dmyc*^{P0}; *hfp*^{EP}/+ stage 14 (H). (I-N) Ovarioles containing stage 10B egg chambers, labelled with BrdU (green) to visualize *chorion* gene amplification and counterstained with the DNA stain propidium iodide (red in L-N). Genotypes: wild type (I,L), *dmyc*^{P1}/*dmyc*^{P1} (J,M), *dmyc*^{P1}/*dmyc*^{P1}; *hfp*^{EP}/+ (K,N). (O-T) Ovarioles containing stage 10 egg chambers, showing in-situ hybridization to *dmyc* mRNA (red) and counterstained with Oligreen. Genotypes: wild type (O,R), *dmyc*^{P0}/*dmyc*^{P0} (P,S), *dmyc*^{P0}/*dmyc*^{P0}; *hfp*^{EP}/+ (Q,T). (U-Z) Analysis of *dmyc* mRNA in third instar wing discs, the ZNC is marked with a yellow bar. (U) wild-type *dmyc* in-situ pattern, (V-Z) *hs-FLP/+; FRT80Bhfp*^{EP}*/FRT80B Tb-GFP*, (V) *hfp*^{EP}/*hfp*^{EP} clones marked by the absence of GFP antibody staining and outlined in white, (W) *dmyc* mRNA expression in *hfp* mutant clones, (X) merged image. (Y,Z) high power images of *hfp*^{EP}/*hfp*^{EP} mutant clones; (Y) GFP antibody staining and (Z) *dmyc* in situ.

genomic endoreplication until stage 10A and switch to amplification of specific loci, including the *chorion* genes at stage 10B (Calvi et al., 1998; Edgar and Orr-Weaver, 2001). Reduced *chorion* gene amplification was observed in *dmyc*^{P1}/*dmyc*^{P1} follicle cells (Fig. 4J,M) compared with the wild-type control (Fig. 4I,L). Consistent with results above, reducing the dosage of *hfp* restored *chorion* gene amplification to normal levels in *dmyc*^{P1}/*dmyc*^{P1} ovaries (Fig. 4K,N).

To test whether increased *dmyc* mRNA was associated with reduced *hfp* gene dosage in ovaries, in-situ hybridization analysis was performed. In wild-type egg chambers, abundant *dmyc* expression was observed in nurse cells and follicle cells (Fig. 4O,R), consistent with previous findings (Gallant et al., 1996). As expected, *dmyc* mRNA abundance was reduced in *dmyc*^{P0}/*dmyc*^{P0} nurse cells compared with wild type, and was almost absent in follicle cells and the oocyte (Fig. 4P,S).

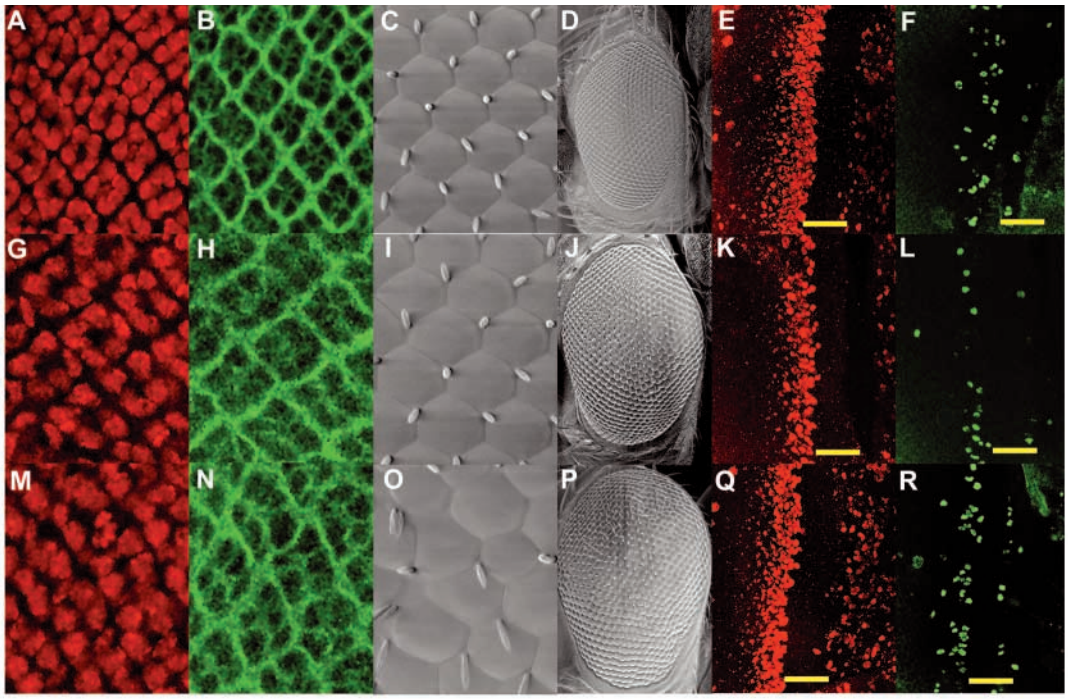

Fig. 5. Hfp negatively regulates G2-M progression. (A-F) Wild type, (G-L) *GMR-GAL4/+*, *UAS-dmyc/+* and (M-R) *GMR-GAL4/+*, *UAS-dmyc/hfp*^{EP}. Cells posterior of the morphogenetic furrow stained with the nuclear stain PI in red (A,G,M) and for cell size with spectrin in green (B,H,N). Scanning electron micrographs showing ommatidia at high power (C,I,O) and the overall size of the adult eye (D,J,P). Analysis of cell cycle progression posterior of the MF in third instar larval eye discs using BrdU (E,K,Q) and anti-phosphohistone H3 (F,L,R). The MF is indicated with a yellow bar.

Increased *dmyc* expression was observed in follicle cells from *dmyc*^{P0}/*dmyc*^{P0}; *hfp*^{EP}/+ egg chambers compared with those from *dmyc*^{P0}/*dmyc*^{P0} flies (Fig. 4Q,T). The relative increase in *dmyc* mRNA in nurse cells of *dmyc*^{P0}/*dmyc*^{P0}; *hfp*^{EP}/+ ovaries is less striking and is likely to be a consequence of cytoplasmic dumping, which is impaired in *dmyc*^{P0}/*dmyc*^{P0} but occurs in *dmyc*^{P0}/*dmyc*^{P0}; *hfp*^{EP}/+ ovaries (see above). These data suggest that, like mammalian FIR, Hfp functions as a negative regulator of *dmyc*.

Hfp mutant clones have elevated *dmyc* expression

To further investigate regulation of *dmyc* expression by Hfp, we generated clones of homozygous *hfp* mutant tissue in wing imaginal tissues using *FLP/FRT*-induced mitotic recombination of the *hfp*^{EP} allele (Xu and Rubin, 1993). Analysis of *hfp* mutant clones revealed reduced levels of staining with the anti-Hfp antibody in third instar eye discs, compared with surrounding non-clonal, GFP-positive tissue (data not shown). Previous mRNA analysis has shown that *dmyc* is expressed in proliferating regions in the wing disc, with lower expression in the non-proliferating ZNC (Johnston et al., 1999). Analysis of mosaic wing discs revealed elevated *dmyc* mRNA expression specifically in *hfp*^{EP} mutant clones, including those spanning the ZNC, compared with surrounding *hfp*^{EP}/+ cells and wild type clones (Fig. 4V-Z). Increased levels of *dmyc* transcript were also observed in *hfp* mutant clones in the eye disc (data not shown); therefore, Hfp acts to repress *dmyc* transcript accumulation in *Drosophila* imaginal tissues.

Hfp negatively regulates *stg*, the rate-limiting factor for G2-M progression

The evidence above suggests that Hfp negatively regulates accumulation of *dmyc* transcript; however, the finding that reducing the dose of *dmyc* does not rescue the *hfp* hypomorphic phenotype (data not shown), suggests that the pupal lethality associated with the *hfp* mutant is not simply a consequence of increased levels of *dmyc*. Therefore, if the *hfp* mutant lethality is not exclusively due to increased *dmyc* expression, Hfp may regulate other essential genes.

Examination of genetic interactions between dMyc and Hfp in the eye also suggested a second role for Hfp. *dmyc* overexpression in wing discs results in larger cells due to increased growth, an accelerated G1 phase and a compensatory extension of G2 phase due to the fact that Cdc25c/Stg, the rate limiting factor for G2-M progression, is not upregulated by dMyc (Johnston et al., 1999). Similarly, overexpression of *dmyc* using the eye driver *GMR-GAL4* results in larger cells posterior to the MF in third instar larvae (Fig. 5G,H compared with wild type, Fig. 5A,B), larger adult ommatidia (Fig. 5I compared with wild type, Fig. 5C) and an oversized adult eye (Fig. 5J compared with wild type, 5D). Reducing the level of *hfp* in this genetic background results in a further increase in the overall size of the *dmyc* overexpressing adult eye (Fig. 5P compared with Fig. 5J) with more disorganized, slightly larger ommatidia (Fig. 5M,N,O compared with Fig. 5G,H,I).

To determine whether cell cycle progression was also affected, we analysed S phase and mitosis in third instar larval eye discs. Assuming that overexpression of *dmyc* affects cell

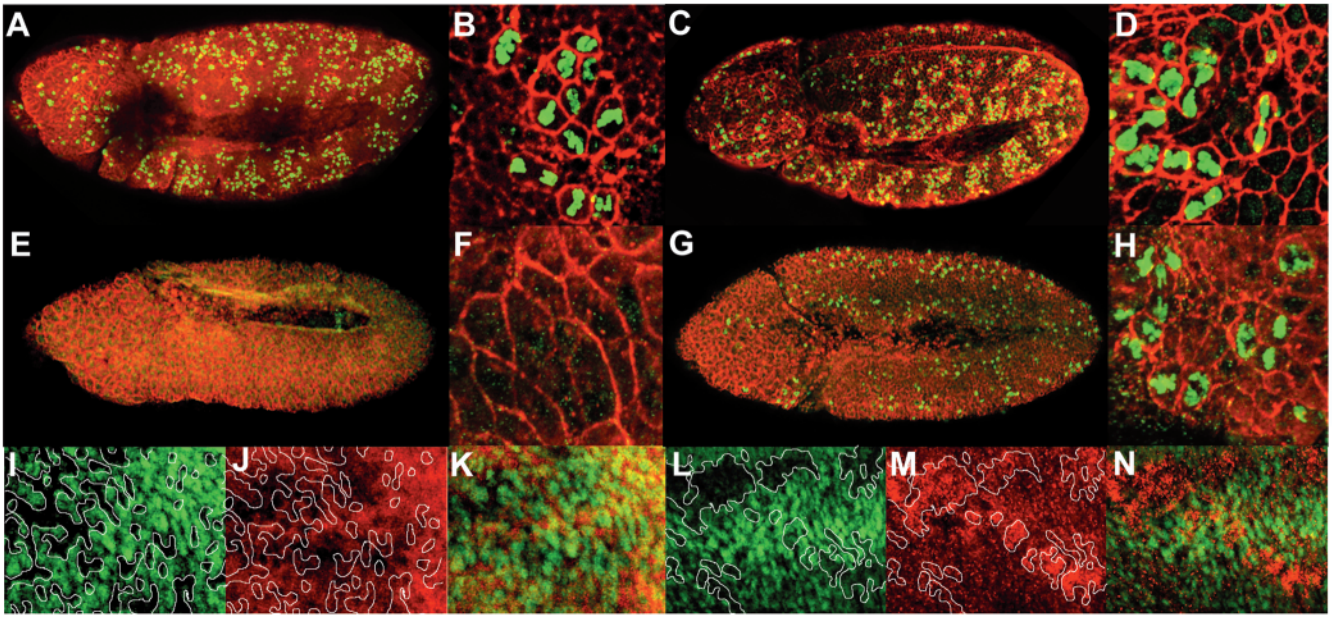

Fig. 6. Hfp negatively regulates Stg. (A-H) Cycle 16 embryos stained with anti-phosphohistone H3 in green to detect mitotic cells and anti-Actin in red to show cell cortex. (A,B) wild type, (C,D) hfp^{EP} mutant embryos (E,F) stg^{AR2} mutant embryos and (G,H) hfp^{EP}, stg^{AR2} double-mutant embryo. (I-N) Wing discs from third instar *hs-FLP; FRT80Bhfp*^{EP}*/FRT80BTb-GFP* flies. (I,L) *hfp* mutant clones are marked by the absence of GFP and outlined in white, (J) in-situ hybridization of *stg* mRNA, (K) in situ merged with GFP, (M) staining with anti-stg antibody and (N) stg-antibody staining merged with GFP.

cycle progression in the eye in a similar manner to that in the wing, it would be expected that eye cells overexpressing *dmyc* would spend more time in G2 and relatively less time in S phase; thus, a thinner S-phase band would result. Indeed, ectopic *dmyc* expression in the posterior part of the eye via *GMR-GAL4* resulted in an S-phase band posterior to the MF that was slightly thinner than wild type (Fig. 5K compared with Fig. 5E). BrdU labelling represents a snap-shot of S phases, and therefore a thinner BrdU band suggests that fewer cells are in S phase at a particular time compared with wild type, consistent with G1-S progression and S phase being accelerated and an extended G2 phase.

Indeed, as expected in the event of a G2 delay, the band of mitotic cells was reduced in *GMR-GAL4*, *UAS-dmyc*/+ eye discs (Fig. 5L compared with wild type, Fig. 5F). Reducing the dose of *hfp* increased both the number of S-phase cells (Fig. 5Q) and restored M-phase entry (Fig. 5R). The increased mitotic cells observed upon reducing the dose of *hfp* suggests that more of the *dmyc* overexpressing G2-delayed cells progress into mitosis. This cannot be explained by the effect of increased *dmyc* levels when *hfp* is reduced and suggests that Hfp may normally negatively regulate a cell cycle component that is required for promotion of G2-M progression.

The increased number of S-phase cells observed upon halving the dose of *hfp* may be a consequence of passage of G2-delayed cells through mitosis into another S phase. To examine the possibility that Hfp might regulate G2-M progression via an inhibitory affect on Stg (the rate limiting regulator of G2-M), we generated hfp^{EP}, stg^{AR2} double mutants and analysed mitoses in mutant embryos using anti-phosphohistone H3 (PH3) staining (Fig. 6A-H). Analysis of hfp^{EP} mutant embryos revealed an apparently normal pattern of PH3 staining in cycle 16 mitotic domains when compared with wild type (Fig. 6C compared with 6A). Closer inspection of the mitotic figures from hfp^{EP} mutant embryos revealed abnormal chromosome morphology; including many lagging chromosomes that are often mis-segregated due to closure of the contractile ring prior to sister chromatid separation (Fig. 6D). Maternal Stg enables mitoses prior to embryonic cycle 14; however, after interphase 14 zygotic transcription of *stg* is required for G2-M progression, and as a consequence *stg* mutants arrest in G2 of cycle 14 (Edgar and O'Farrell, 1990). As expected, cycle 14 stg^{AR2} mutant embryos lacked PH3 staining (Fig. 6E), and were comprised solely of large G2 cells (Fig. 6F). Strikingly, mitotic entry was restored in hfp^{EP}, stg^{AR2} double mutant embryos (Fig. 6G), and consequently cell size was restored to the wild type range (Fig. 6H). Furthermore, in contrast to the complete embryonic lethality of *stg* mutant embryos, hfp^{EP}, stg^{AR2} double mutants survive embryogenesis and die between first and second instar. Thus, in addition to negatively regulating *dmyc* and G1-S progression, these results suggests that Hfp normally acts to negatively regulate mitotic entry via negative regulation of *stg*.

The *stg* mutant used in the above experiment is a null, which suggests that Hfp affects accumulation or stability of the maternally supplied *stg* transcript or Stg protein, which are both normally actively degraded prior to cycle 14 of embryogenesis. In-situ hybridization to *hfp* mutant wing clones, using a DIG labelled *stg* probe (Fig. 6I-K), revealed no difference between levels of *stg* mRNA in clonal tissue. This suggests that the affect on *stg* is not via Hfp stabilizing *stg* mRNA. However, using an Stg antibody, we found increased levels of Stg protein in *hfp* mutant clones (Fig. 6L-N), suggesting that Hfp might normally regulate factors required for Stg translation or protein degradation.

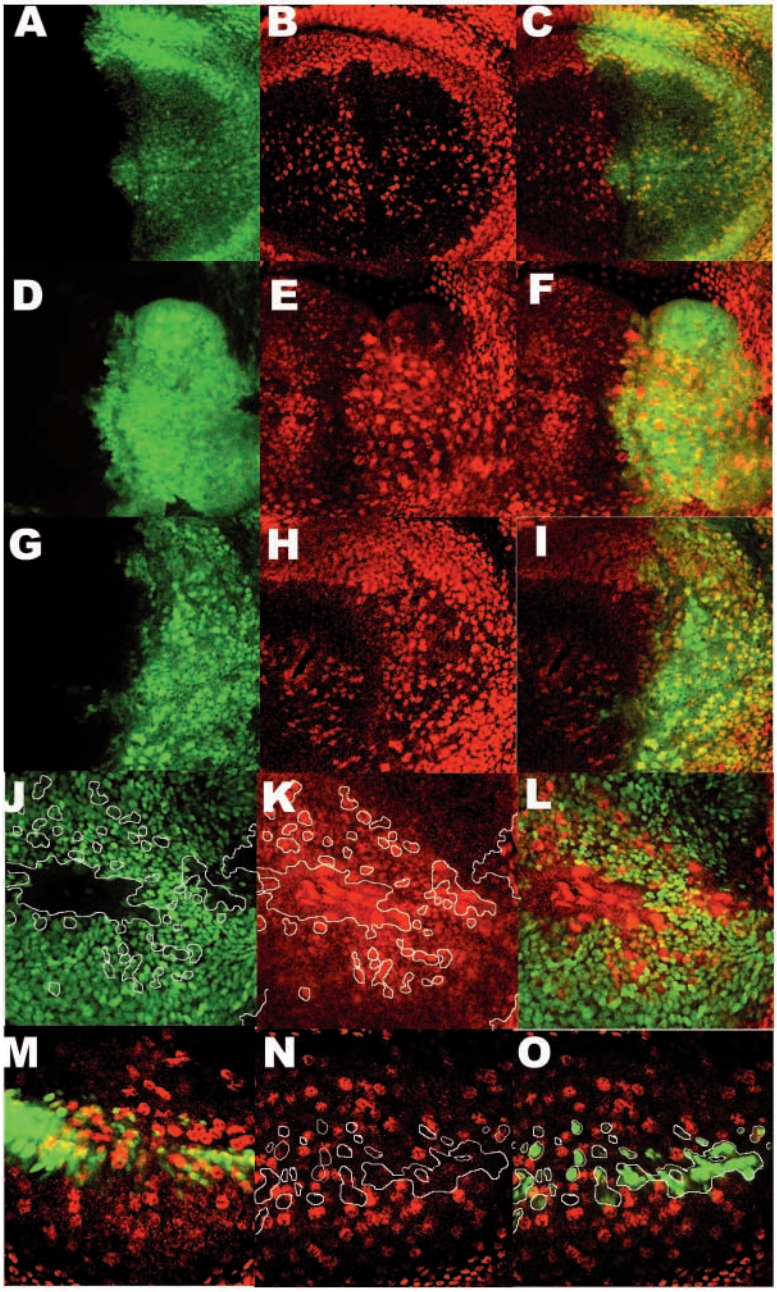

Fig. 7. Activation of the Wg pathway causes induction of Hfp in wing discs. Hfp expression in wing discs from larvae of the following genotypes: *en-GAL4/+,UAS-GFP/+* (A-C), *en-GAL4/+, UAS-GFP/+;UAS-hfp/+* (D-F), *en-GAL4/+,UAS-GFP/+;UAS-sgg^{DN}/+* (G-I). (A,D,G), GFP (green) marks the posterior region of the wing disc, (B,E,H) anti-Hfp antibody staining (red), and (G,F,I) are merged images. (J-L) Hfp expression in *axin* mutant clones from third instar wing discs, (J) clones marked by the absence of GFP, (K) anti-Hfp antibody staining and (L) merged image. (M) Hfp expression and GFP in the ZNC of control *C96-GAL4/+, UAS-GFP/+* wing discs, (N) Hfp expression in *C96-GAL4/+, UAS-GFP/+, UAS-TCF^{DN}/+* and (O) merge with GFP.

Wg patterning regulates Hfp expression

The cell cycle arrest and repression of *dmyc* normally observed in the wing disc ZNC requires Wg expression and a functional Wg pathway (Johnston and Edgar, 1998). Hence, expression of a dominant negative form of TCF (TCF^{DN}) in cells of the ZNC causes ectopic induction of *dmyc* and cell cycle entry (Johnston et al., 1999). As both *dmyc* expression and cell proliferation in the wing disc appear to be inhibited by Hfp, we hypothesized that Hfp expression may be under the control of the Wg pathway. To test this, we activated the Wg pathway in the posterior compartment of the wing disc by expressing a dominant negative form of Shaggy, Sgg^{DN}, using the *en-GAL4* driver. Shaggy is the *Drosophila* orthologue of vertebrate glycogen synthase kinase 3 (GSK3), an inhibitory component of the Wg signalling pathway (Siegfried et al., 1992). Therefore, expression of the dominant negative transgene (Sgg^{DN}) results in ectopic activation of the Wg signalling pathway. As expected, control *en-GAL4,UAS-GFP* larval wing discs showed GFP expression restricted to the posterior region of the disc and ubiquitous staining for Hfp (Fig. 7A-C). Increased staining with the anti-Hfp antibody was observed in the posterior region of *en-GAL4,UAS-hfp* wing discs as expected (Fig. 7D-F). Significantly, activation of the Wg pathway by Sgg^{DN} resulted in similar high levels of ectopic Hfp expression in the posterior region of the wing disc (Fig. 7G-I). To further confirm that Hfp is upregulated by Wg signalling, we analysed *axin* mutant clones, in which the Wg pathway is constitutively active, since Axin normally downregulates Armadillo (Hamada et al., 1999). Indeed, increased Hfp protein was observed in *d-axin* mutant clones, marked by the absence of GFP (Fig. 7J-L). Conversely, when Wg signalling was blocked by expressing a dominant negative form of TCF (TCF^{DN}) in the ZNC using the *C96-GAL4* driver (Johnston et al., 1999) Hfp protein was reduced in all TCF^{DN} expressing cells, which are marked by coexpression of GFP (Fig. 7N,O, compared with the normal high level of Hfp in ZNC cells from wild type, Fig. 7M). Reduced numbers of ZNC cells (i.e. fewer cells stained for GFP) are observed as a consequence of TCF^{DN} overexpression, since cells die by apoptosis when Wg signalling is blocked (Johnston and Sanders, 2003). Therefore, ectopic activation of the Wg pathway is associated with increased levels of Hfp in the wing disc, and blocking Wg signalling reduces Hfp expression. Taken together, these results show that ectopic activation of the Wg pathway increases the level of Hfp in third instar wing discs, consistent with the notion that Wg may normally act by inducing *hfp* to inhibit *dmyc* expression in the ZNC.

Discussion

Hfp negatively regulates G1-S progression, via downregulation of *dmyc*

In this study we have shown that Hfp is a negative regulator of cell cycle entry in *Drosophila* as evidenced by: (1) ectopic S phases in the ZNC of *hfp* mutant wing discs and increased S phase in the second mitotic wave in the eye disc; (2) inhibition of S phases in larval imaginal tissues by overexpression of the

UAS-hfp transgene; and (3) dominant suppression of the *GMR*-driven human *p21* or *dacapo* rough eye phenotypes and rescue of the posterior band of S phases in *GMR-p21* eye discs by reducing the level of *hfp*. These data suggest that Hfp normally has a role in preventing S-phase entry in cells destined to differentiate in the eye and wing imaginal discs. Furthermore, we show that this negative regulation of the cell cycle by Hfp is partly a consequence of inhibitory affects on *dmyc*, since: (1) an increased level of *dmyc* mRNA transcript occurred in *hfp–/–* clones; and (2) reduced levels of Hfp could rescue the *dmyc* mutant ovary phenotype, by restoring levels of *dmyc* mRNA to more wild-type levels. Indeed, upregulation of *dmyc* expression in Hfp mutants may explain the rescue of S phases in eye discs overexpressing p21 or Dacapo, consistent with the observation that *dmyc* mutants dominantly enhance the *GMR-p21* and *GMR*-driven *dacapo* rough eye phenotypes (Fig. 3). Mammalian Myc stimulates *cyclin E* expression, activation of Cdks (Bouchard et al., 1999), antagonizes the action of Cdk inhibitors, including p27 (Vlach et al., 1996; O'Hagan et al., 2000), and can downregulate *p21* transcription (Claassen and Hann, 2000; Gartel et al., 2001) and p21 activity via direct c-Myc-p21 protein–protein interaction (Kitaura et al., 2000). In *Drosophila*, dMyc has been shown to lead to an increase in Cyclin E protein levels by a post-transcriptional mechanism (Prober and Edgar, 2002), which by itself could explain the suppression of the *GMR-p21* eye phenotype by reducing the dose of *hfp*. Whether dMyc can also inhibit p21 or Dacapo activity in *Drosophila* is unknown.

Dual function for Hfp in regulation of splicing and *dmyc* transcription?

Increased levels of *dmyc* transcript were observed in *hfp* mutant clones, consistent with Hfp acting to repress *dmyc* transcript accumulation in *Drosophila* imaginal tissues. The upregulation of *dmyc* mRNA in *hfp* mutant tissue could occur through alterations in *dmyc* transcription (initiation or elongation), pre-mRNA splicing, mRNA message stability or a combination of these processes. Mammalian FIR was first shown to regulate pre-mRNA splicing by binding to RNA polypyrimidine tracts and cooperating with the essential splicing factor U2AF (Page-McCaw et al., 1999). Consistent with this, recent studies in *Drosophila* show that the FIR orthologue Hfp is required for correct splicing of several genes in the developing ovary (Van Buskirk and Schupbach, 2002). Mammalian FIR has been shown to have a second role as transcriptional repressor of *Myc*, through first forming a complex with the *Myc* activator FBP and interfering with the basal transcription apparatus by then binding TFIIH, thereby disrupting helicase function (Liu et al., 2000). The data described here suggest that the cell cycle inhibitory function of Hfp is partly a consequence of negatively regulating *dmyc* expression. Therefore, the dual roles of transcription regulation and mRNA splicing appear to have been evolutionarily conserved between *Drosophila* Hfp and mammalian FIR. It remains to be determined whether Hfp inhibits *dmyc* expression by a mechanism analogous to the mammalian FIR/FBP/FUSE interaction. A FUSE element has not been identified upstream of the *dmyc* promoter, and although the *Drosophila* splicing factor PSI is a highly conserved orthologue of FBP (Labourier et al., 2002), it has not been reported whether PSI can activate *dmyc* expression.

Hfp regulates G2-M progression, via negative regulation of *stg*

Our finding that *hfp* mutants do not phenocopy *dmyc* overexpression suggested that inhibition of *dmyc* expression is not the only role of Hfp. Although increased S phases are observed in *hfp* mutant wing discs, this is not associated with increased cell size, as occurs with *dmyc* overexpression in the wing disc. Rather, in *hfp* mutant wing discs the ZNC, which normally contains domains of G1- and G2-arrested cells (Johnston and Edgar, 1998), has ectopic S-phase and M-phase cells. Since cells in *hfp* mutant wing discs are of normal size and ectopically enter S phase, it is possible that progression through G2 may also be accelerated. Indeed, the increased number of mitotic cells observed in eye imaginal discs when the level of Hfp is reduced in a *dmyc* overexpression background, suggests that Hfp normally negatively regulates G2-M phase progression. Furthermore, the abnormal mitotic figures observed in hfp^{EP} mutant embryos are consistent with accelerated cell cycle progression (Quinn et al., 2001). Most importantly, the *hfp* mutant rescued the cycle 14 G2-arrest that normally occurs in *stg* mutant embryos, and *hfp* mutant clones have increased levels of Stg protein, suggesting that Hfp normally exerts an inhibitory affect on G2-M progression via negatively regulating Stg translation or protein stability. Thus, Hfp may be required for negatively regulating both the G1-S phase transition by downregulating *dmyc* and the G2-M transition by negatively regulating *stg*.

Regulation of Hfp, dMyc and Stg by the Wingless pathway

The Wg pathway is required to downregulate both *dmyc* and *stg*

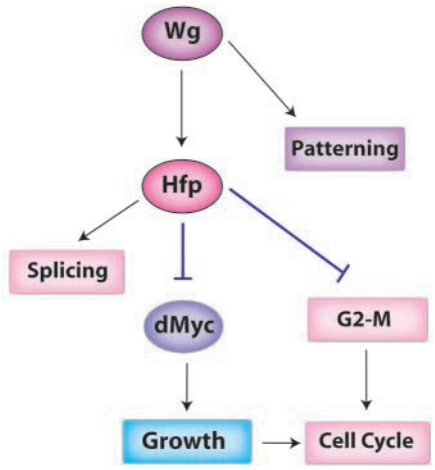

Fig. 8. Model for Wg signalling through Hfp during *Drosophila* development. The Wg signalling pathway has a role in tissue patterning and is also required to downregulate *dmyc* expression and limit cell proliferation in the ZNC during wing development via repression of *dmyc* expression (Johnston et al., 1999). Our results suggest that Hfp may link Wg signalling to the control of cell growth and proliferation by repressing dMyc expression (see text). Wg signalling is also required to induce the domain of G2-arrested cells in the ZNC, via upregulation of *achaete* and *scute*, which in turn downregulate *stg* (Johnston and Edgar, 1998). Our data is consistent with Wg signalling upregulating Hfp, which would then play a role in negatively regulating *stg* post-transcriptionally and thereby leading to a G2-arrest.

expression in order to limit cell proliferation in the ZNC during wing development (Johnston and Edgar, 1998; Johnston et al., 1999). Activation of the Wg pathway, using either dominant negative Shaggy or by generation of *axin* clones, resulted in a strong and specific increase in Hfp protein, demonstrating that Wg pathway activation is sufficient to cause Hfp induction. Our findings supported a model in which Wg signalling causes induction of Hfp in the wing disc ZNC, which in turn inhibits *dmyc* expression (to elicit the posterior, G1 arrest) and *stg* expression or activity (to provide the anterior, G2-arrested domains) (Fig. 8). The involvement of Achaete and Scute in this process, which have been previously shown to play a role in the negative regulation of *stg* (Johnston and Edgar, 1998) remains to be elucidated. Previous studies have shown that Ras signalling through Raf/MAPK upregulates *dmyc* post-transcriptionally in wing disc cells and is required to maintain normal dMyc protein levels in the wing disc (Prober and Edgar, 2000; Prober and Edgar, 2002). In contrast, since *hfp* clones have increased *dmyc* mRNA, Hfp must normally inhibit *dmyc* mRNA accumulation. Furthermore, overexpression of Hfp inhibits cell proliferation in all wing and eye imaginal discs, suggesting that Hfp may normally override mitogenic signals and lead to cell cycle arrest during particular stages of development.

In summary, our results suggested that Hfp negatively regulates cell proliferation by inhibiting *dmyc* transcription and Stg protein accumulation. Hfp is required for the developmentally regulated cell cycle arrest within the ZNC and is responsive to the Wg signalling pathway that regulates this arrest, suggesting that Hfp links patterning signals to cell proliferation during *Drosophila* development.

We thank Trudi Schupbach for anti-Hfp antibody, Laura Johnston for the *UAS-TCF^{DN}* and *en-GAL4,UAS-GFP* strains and for critical reading of the manuscript, Iswar Hariharan for the *GMR-p21* strain, Jessica Treisman for the *axin*, *FRT82B* stock and Bruce Edgar for the anti-Stg antibody, *stg* cDNA and *C96-GAL4* fly strain. We thank Grant McArthur, David Levens, and Izhak Haviv for critical reading of the manuscript, and members of the Bowtell and Richardson labs for helpful discussions. G.R.H., D.D.L.B. and H.R. are supported by grants from the Australian National Health and Medical Research Council. H.R. is a Wellcome Senior Research Fellow in Medical Science.

References

Asano, M., Nevins, J. R. and Wharton, R. P. (1996). Ectopic E2F expression induces S phase and apoptosis in Drosophila imaginal discs. *Genes Dev*. **10**, 1422-1432.

Bouchard, C., Thieke, K., Maier, A., Saffrich, R., Hanley-Hyde, J., Ansorge, W., Reed, S., Sicinski, P., Bartek, J. and Eilers, M. (1999). Direct induction of cyclin D2 by Myc contributes to cell cycle progression and sequestration of p27. *EMBO J*. **18**, 5321-5333.

Buszczak, M. and Cooley, L. (2000). Eggs to die for: cell death during Drosophila oogenesis. *Cell Death Differ*. **7**, 1071-1074.

Calvi, B. R., Lilly, M. A. and Spradling, A. C. (1998). Cell cycle control of chorion gene amplification. *Genes Dev*. **12**, 734-744.

Claassen, G. F. and Hann, S. R. (2000). A role for transcriptional repression of p21CIP1 by c-Myc in overcoming transforming growth factor beta-induced cell-cycle arrest. *Proc. Natl. Acad. Sci. USA* **97**, 9498-9503.

de Nooij, J. C. and Hariharan, I. K. (1995). Uncoupling cell fate determination from patterned cell division in the Drosophila eye. *Science* **270**, 983-985.

Dorstyn, L., Colussi, P. A., Quinn, L. M., Richardson, H. and Kumar, S. (1999). DRONC, an ecdysone-inducible Drosophila caspase. *Proc. Natl. Acad. Sci. USA* **96**, 4307-4312.

Duncan, R., Bazar, L., Michelotti, G., Tomonaga, T., Krutzsch, H., Avigan, M. and Levens, D. (1994). A sequence-specific, single-strand binding protein activates the far upstream element of Myc and defines a new DNA-binding motif. *Genes Dev*. **8**, 465-480.

Edgar, B. A. and O'Farrell, P. H. (1989). Genetic control of cell division patterns in the Drosophila embryo. *Cell* **57**, 177-187.

Edgar, B. A. and O'Farrell, P. H. (1990). The three postblastoderm cell cycles of Drosophila embryogenesis are regulated in G2 by string. *Cell* **62**, 469-480.

Edgar, B. A. and Orr-Weaver, T. L. (2001). Endoreplication cell cycles: more for less. *Cell* **105**, 297-306.

Edgar, B. A., Sprenger, F., Duronio, R. J., Leopold, P. and O'Farrell, P. H. (1994). Distinct molecular mechanism regulate cell cycle timing at successive stages of Drosophila embryogenesis. *Genes Dev*. **8**, 440-452.

Eisenman, R. N. (2001). Deconstructing myc. *Genes Dev*. **15**, 2023-2030.

Gallant, P., Shiio, Y., Cheng, P. F., Parkhurst, S. M. and Eisenman, R. N. (1996). Myc and Max homologs in Drosophila. *Science* **274**, 1523-1527.

Gartel, A. L., Ye, X., Goufman, E., Shianov, P., Hay, N., Najmabadi, F. and Tyner, A. L. (2001). Myc represses the p21(WAF1/CIP1) promoter and interacts with Sp1/Sp3. *PNAS* **98**, 4510-4515.

Gutzeit, H. O. (1986). The role of microfilaments in cytoplasmic streaming in Drosophila follicles. *J. Cell Sci*. **80**, 159-169.

Hamada, F., Tomoyasu, Y., Takatsu, Y., Nakamura, M., Nagai, S., Suzuki, A., Fujita, F., Shibuya, H., Toyoshima, K., Ueno, N. et al. (1999). Negative regulation of Wingless signaling by D-axin, a Drosophila homolog of axin. *Science* **283**, 1739-1742.

Hans, F. and Dimitrov, S. (2001). Histone H3 phosphorylation and cell division. *Oncogene* **20**, 3021-3027.

He, L., Liu, J., Collins, I., Sanford, S., O'Connell, B., Benham, C. J. and Levens, D. (2000). Loss of FBP function arrests cellular proliferation and extinguishes c-myc expression. *EMBO J*. **19**, 1034-1044.

Johnston, L. A. and Edgar, B. A. (1998). Wingless and Notch regulate cell-cycle arrest in the developing Drosophila wing. *Nature* **394**, 82-84.

Johnston, L. A. and Sanders, A. L. (2003). Wingless promotes cell survival but constrains growth during Drosophila wing development. *Nat. Cell Biol*. **5**, 827-833.

Johnston, L. A., Prober, D. A., Edgar, B. A., Eisenman, R. N. and Gallant, P. (1999). Drosophila myc regulates cellular growth during development. *Cell* **98**, 779-790.

Kitaura, H., Shinshi, M., Uchikoshi, Y., Ono, T., Tsurimoto, T., Yoshikawa, H., Iguchi-Ariga, S. M. M. and Ariga, H. (2000). Reciprocal Regulation via Protein-Protein Interaction between c-Myc and p21cip1/waf1/sdi1 in DNA Replication and Transcription. *J. Biol. Chem*. **275**, 10477-10483.

Kornberg, T., Siden, I., O'Farrell, P. and Simon, M. (1985). The engrailed locus of Drosophila: in situ localization of transcripts reveals compartment-specific expression. *Cell* **40**, 45-53.

Labourier, E., Blanchette, M., Feiger, J. W., Adams, M. D. and Rio, D. C. (2002). The KH-type RNA-binding protein PSI is required for Drosophila viability, male fertility, and cellular mRNA processing. *Genes Dev*. **16**, 72-84.

Liu, J., Akoulitchev, S., Weber, A., Ge, H., Chuikov, S., Libutti, D., Wang, X. W., Conaway, J. W., Harris, C. C., Conaway, R. C. et al. (2001). Defective interplay of activators and repressors with TFIH in xeroderma pigmentosum. *Cell* **104**, 353-363.

Liu, J., He, L., Collins, I., Ge, H., Libutti, D., Li, J., Egly, J. and Levens, D. (2000). The FBP interacting repressor targets TFIIH to inhibit activated transcription. *Mol. Cell* **5**, 331-341.

Neufeld, T. P., de la Cruz, A. F., Johnston, L. A. and Edgar, B. A. (1998). Coordination of growth and cell division in the Drosophila wing. *Cell* **93**, 1183-1193.

O'Hagan, R. C., Ohh, M., David, G., de Alboran, I. M., Alt, F. W., Kaelin, W. G., Jr and DePinho, R. A. (2000). Myc-enhanced expression of Cul1 promotes ubiquitin-dependent proteolysis and cell cycle progression. *Genes Dev*. **14**, 2185-2191.

Page-McCaw, P. S., Amonlirdviman, K. and Sharp, P. A. (1999). PUF60: a novel U2AF65-related splicing activity [In Process Citation]. *RNA* **5**, 1548-1560.

Poleev, A., Hartmann, A. and Stamm, S. (2000). A trans-acting factor, isolated by the three-hybrid system, that influences alternative splicing of the amyloid precursor protein minigene. *Eur. J. Biochem*. **267**, 4002-4010.

Prober, D. A. and Edgar, B. A. (2000). Ras1 promotes cellular growth in the Drosophila wing. *Cell* **100**, 435-446.

Prober, D. A. and Edgar, B. A. (2002). Interactions between Ras1, dMyc,

and dPI3K signaling in the developing Drosophila wing. *Genes Dev*. **16**, 2286-2299.

Quinn, L. M., Dorstyn, L., Mills, K., Colussi, P. A., Chen, P., Coombe, M., Abrams, J., Kumar, S. and Richardson, H. (2000). An essential role for the caspase dronc in developmentally programmed cell death in Drosophila. *J. Biol. Chem.* **275**, 40416-40424.

Quinn, L. M., Herr, A., McGarry, T. J. and Richardson, H. (2001). The Drosophila Geminin homolog: roles for Geminin in limiting DNA replication, in anaphase and in neurogenesis. *Genes Dev*. **15**, 2741-2754.

Richardson, H., O'Keefe, L. V., Marty, T. and Saint, R. (1995). Ectopic cyclin E expression induces premature entry into S phase and disrupts pattern formation in the Drosophila eye imaginal disc. *Development* **121**, 3371-3379.

Rio, D. (2002). Half-pint: alternative splicing in the Drosophila ovary. *Mol. Cell* **9**, 456-457.

Schreiber-Agus, N., Stein, D., Chen, K., Goltz, J. S., Stevens, L. and DePinho, R. A. (1997). Drosophila Myc is oncogenic in mammalian cells and plays a role in the diminutive phenotype. *Proc. Natl. Acad. Sci. USA* **94**, 1235-1240.

Secombe, J., Pispa, J., Saint, R. and Richardson, H. (1998). Analysis of a Drosophila cyclin E hypomorphic mutation suggests a novel role for cyclin E in cell proliferation control during eye imaginal disc development. *Genetics* **149**, 1867-1882.

Siegfried, E., Chou, T. B. and Perrimon, N. (1992). wingless signaling acts through zeste-white 3, the Drosophila homolog of glycogen synthase kinase-3, to regulate engrailed and establish cell fate. *Cell* **71**, 1167-1179.

Van Buskirk, C. and Schupbach, T. (2002). Half pint regulates alternative splice site selection in Drosophila. *Dev. Cell* **2**, 343-353.

Vlach, J., Hennecke, S., Alevizopoulos, K., Conti, D. and Amati, B. (1996). Growth arrest by the cyclin-dependent kinase inhibitor p27Kip1 is abrogated by c-Myc. *EMBO J.* **15**, 6595-6604.

Xu, T. and Rubin, G. M. (1993). Analysis of genetic mosaics in developing and adult Drosophila tissues. *Development* **117**, 1223-1237.